Model Predictive Control for Blending Processes in Cement Plants

Zhanhao Zhang [*,**] **Marcus Krogh Nielsen** [*,**]
Guruprasath Muralidharan [***] **Steen Hørsholt** [*,**]
John Bagterp Jørgensen [*,**]

[*] *Department of Applied Mathematics and Computer Science*
Technical University of Denmark, DK-2800 Kgs. Lyngby, Denmark
[**] *2-control ApS, Copenhagen, Denmark*
[***] *Smarta-Opti Solutions, Chennai, India*

Abstract: In this paper, we discuss model predictive control applied to blending processes. Blending processes are ubiquitous in the chemical process industries since reactants usually need to be mixed before entering a reactor. Many times, the blending is trivial as pure streams of reactants are mixed. We consider non-trivial blending problems in which non-pure streams with the reactants are to be mixed. The motivating example is the blending problem that occurs in cement production. The raw mix for the cement kiln must have a specified chemical composition. This composition is obtained by mixing piles with different chemical compositions and economic value such that the raw mix meets specifications in the cheapest possible way. We formulate the blending problem as a nonlinear optimization problem that can be approximated well as a convex quadratic optimization problem. We implement the corresponding nonlinear and linear model predictive controllers (NMPC, LMPC) using a continuous-time transfer function description that is realized as a discrete-time linear state space model. The controller obtains feedback by combining regularly sampled online measurements and irregularly sampled laboratory measurements using a time variant dynamic Kalman filter with memory. Numerical simulations demonstrate that the NMPC and LMPC have similar performance.

Keywords: Advanced Process Control, Model Predictive Control, Blending, Cement Processes

1. INTRODUCTION

With the growth of the construction industry, global cement production has doubled in the last decade, peaking at 4.2 Gt in 2016. The rapid growth of cement production has brought more carbon emissions, accounting for approximately 7% of the global CO_2 emission (Robbie, 2019). To develop a sustainable cement industry, research related electrification, carbon capture and storage (CCS), as well as digitalization and optimization of the cement manufacturing process is needed. In this paper, we contribute to the digitalization, control and optimization of cement manufacturing by describing nonlinear and linear model predictive control for cement raw material blending.

1.1 Cement manufacturing and raw material blending

The cement manufacturing process consists of four phases: raw material quarrying, raw mix blending, clinker burning, and cement mill grinding. The purpose of the raw mix blending process is to guarantee that the output raw meal meets certain quality standards. The raw mix blending process needs to be well controlled since the quality of the raw meal directly influences the cement quality. Figure 1 shows a diagram of the raw mix blending process. The raw mix blending process starts with the transportation of raw materials. Limestone, clay, and other raw materials from raw material piles are fed to the raw mill by conveyor belts. In the raw mill, raw materials are blended and ground into particles of a desired size. The final output from the raw mill is denoted as raw meal. Finally, a conveyor belt transports the output raw meal to a homogenization silo. The quality standards of the raw meal are determined by the oxide composition of the raw meal. Online X-ray sensors and laboratory analyzes are used to determine the composition of the raw meal. Compared to online measurements, the processing time is longer and the sampling frequency is lower for laboratory measurements, but the latter has more accurate measurement results. Therefore, it is necessary to address the problem of including measurements with delays, different frequencies, and even missing observations. In this paper, we consider three compositional parameters: lime saturation factor (LSF), alumina modulus (ALM), and silica modulus (SIM). These compositional parameters are nonlinear functions of the concentration of the four main oxide components: SiO_2 (Si), Al_2O_3 (Al), Fe_2O_3 (Fe), and CaO (Ca). This paper focuses on optimal control of the compositional parameters for the raw mix blending process.

1.2 Model predictive control for uncertain systems

In the raw mix blending process, the model uncertainty caused by the variation in raw material pile composition must be considered. Vinicius et al. (2015) introduce a

[1] Corresponding author: J.B. Jørgensen (e-mail: jbjo@dtu.dk)

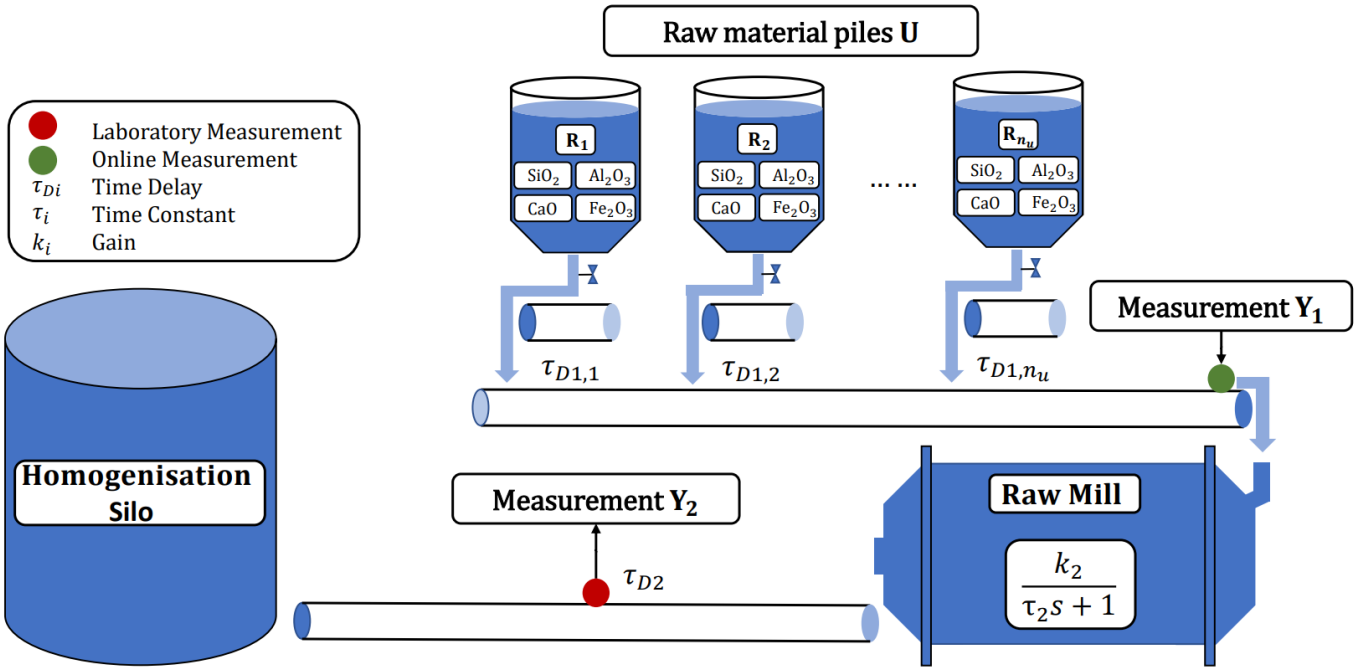

Fig. 1. The cement raw mix blending process. The green dot indicates the online measurement point Y_1. The red dot is the laboratory measurement point Y_2. $\tau_{D1,i}$ for $i \in \{1, 2, \ldots, n_u\}$ are the time delays between the i'th pile and the online measurement point Y_1. τ_{D2} indicates the time delay between Y_1 to Y_2. k_2 and τ_2 indicate the gain and time constant of the raw mill transfer function model.

linear parameter varying (LPV) system for modeling the raw mix blending process, where the model uncertainty is presented in a set of uncertain parameters. They describe a robust gain-scheduled control method, which can effectively control the raw mix blending process. Prasath et al. (2010) describe a soft constrained model predictive control (MPC) algorithm for an industrial cement mill grinding process. The proposed soft constrained MPC can handle the plant-model mismatch. Due to the nonlinearity of the compositional parameters, the linear MPC (LMPC) algorithm cannot be directly applied to the reference tracking objective. This paper presents a soft constrained LMPC based on a novel formulation of the blending optimization problem. Furthermore, a Kalman filter with memory is introduced for handling missing and delayed measurements. This paper demonstrates through a numerical experiment that the proposed LMPC performs similarly to a nonlinear MPC (NMPC) for reference tracking and disturbance rejection related to variations in the chemical composition of the piles.

1.3 Paper organization

This paper is organized as follows. Section 2 describes the dynamics and modeling of the raw mix blending process. Section 3 illustrates a linear discrete-time dynamic Kalman filter with memory. Section 4 describes a novel formulation of the blending optimal control problem, where it is approximated as a convex quadratic program (QP). The comparison between the proposed LMPC and an NMPC is provided and discussed in Section 5. Conclusions are given in Section 6.

2. SYSTEM MODELING

Figure 1 illustrates the cement raw mix blending process considered in this paper. We assume the total system feed rate F [t/h] is fixed. The feed fractions of the individual raw material piles are manipulated variables (MVs). Therefore, the system input $u(t)$ is defined as

$$u(t) = [u_1(t); u_2(t); \ldots; u_{n_u}(t)], \quad e^T u(t) = 1. \tag{1}$$

$u_i(t)$ for $i \in \{1, 2, \ldots, n_u\}$ indicates the feed fraction of the i'th pile. $e = [1; 1; \ldots; 1]$ is a unit vector, such that $\sum_{i=1}^{n_u} u_i(t) = e^T u(t) = 1$.

The composition of the raw material piles are represented by the compositional matrix P, and the corresponding unit costs [\$/t] are represented by the cost vector c, i.e.

$$P = \begin{bmatrix} \mathrm{Si}_1 & \mathrm{Si}_2 & \cdots & \mathrm{Si}_{n_u} \\ \mathrm{Al}_1 & \mathrm{Al}_2 & \cdots & \mathrm{Al}_{n_u} \\ \mathrm{Fe}_1 & \mathrm{Fe}_2 & \cdots & \mathrm{Fe}_{n_u} \\ \mathrm{Ca}_1 & \mathrm{Ca}_2 & \cdots & \mathrm{Ca}_{n_u} \end{bmatrix}, \qquad c = \begin{bmatrix} c_1 \\ c_2 \\ \vdots \\ c_{n_u} \end{bmatrix}. \tag{2}$$

Si_i, Al_i, Fe_i, Ca_i, c_i represent oxide element concentrations and the cost of i'th pile, respectively.

The controlled variables (CVs) of the blending process are considered as the concentration of oxide components at two measurement points. Therefore, the system output $Z(t)$ is defined as

$$Z(t) = \begin{bmatrix} Z_1(t) \\ Z_2(t) \end{bmatrix}, \quad Z_i(t) = \begin{bmatrix} \mathrm{Si}_{z,i}(t) \\ \mathrm{Al}_{z,i}(t) \\ \mathrm{Fe}_{z,i}(t) \\ \mathrm{Ca}_{z,i}(t) \end{bmatrix}, \quad i \in \{1, 2\}. \tag{3}$$

The raw mix blending process can be described by two coupled input-output models, and they can be expressed on standard form as

$$\begin{bmatrix}\boldsymbol{Z}_1(s)\\ \boldsymbol{Z}_2(s)\end{bmatrix} = \begin{bmatrix}G_{D1}(s)\\ \bar{G}_{D2}(s)\end{bmatrix} U(s) + \begin{bmatrix}H_1(s) & 0\\ H_{21}(s) & H_2(s)\end{bmatrix} \begin{bmatrix}\boldsymbol{W}_1(s)\\ \boldsymbol{W}_2(s)\end{bmatrix}, \tag{4a}$$

$$\begin{bmatrix}\boldsymbol{Y}_1(s)\\ \boldsymbol{Y}_2(s)\end{bmatrix} = \begin{bmatrix}\boldsymbol{Z}_1(s)\\ \boldsymbol{Z}_2(s)\end{bmatrix} + \begin{bmatrix}\boldsymbol{V}_1(s)\\ \boldsymbol{V}_2(s)\end{bmatrix}, \tag{4b}$$

where

$$G_{D1}(s) = PT(s), \qquad G_{D2}(s) = \frac{k_2}{\tau_2 s+1} e^{-\tau_{D2} s}, \tag{5a}$$

$$H_1(s) = \frac{k_{H1}}{\tau_{H1} s+1}, \qquad H_2(s) = \frac{k_{H2}}{\tau_{H2} s+1}, \tag{5b}$$

$$\bar{G}_{D2}(s) = G_{D2}(s) G_{D1}(s),\ H_{21}(s) = G_{D2}(s) H_1(s), \tag{5c}$$

$G_{D1}(s)$, and $\bar{G}_{D2}(s)$ are transfer functions for the deterministic system dynamics from the MVs (U) to the outputs (Z). $G_{D1}(s)$ indicates the dynamics from raw material piles to the online measurement point Y_1, where $T(s) = \text{diag}([e^{-\tau_{D1,1}s}; e^{-\tau_{D1,2}s}; \ldots; e^{-\tau_{D1,n_u}s}])$ are input time delays. The deterministic dynamics from the online measurement point Y_1 to the laboratory measurement point Y_2 is given by $G_{D2}(s) = G_2(s)e^{-\tau_{D2}s}$; the raw mill transfer function, $G_2(s) = k_2/(\tau_2 s + 1)$ (with $k_2 = 1$) and the conveyor belt transportation delay, $e^{-\tau_{D2}s}$. $H_1(s)$ and $H_2(s)$ are transfer functions for the stochastic system dynamics, i.e. the dynamics from the process noise (W) to the outputs (Z). $\boldsymbol{W}_1(s)$ and $\boldsymbol{W}_2(s)$ are inputs representing system uncertainties and modeled as standard Wiener processes. The measurements, $\boldsymbol{Y}_1(s)$ and $\boldsymbol{Y}_2(s)$, are the system outputs, $\boldsymbol{Z}_1(s)$ and $\boldsymbol{Z}_2(s)$, corrupted by additive Gaussian measurement noise, $\boldsymbol{V}_1(s)$ and $\boldsymbol{V}_2(s)$.

The input-output model is realized as a discrete-time state space model [2]

$$\boldsymbol{x}_{k+1} = A\boldsymbol{x}_k + Bu_k + G\boldsymbol{w}_k, \quad \boldsymbol{w}_k \sim \mathcal{N}_{iid}(0, Q), \tag{6a}$$

$$\boldsymbol{z}_k = C\boldsymbol{x}_k, \tag{6b}$$

$$\boldsymbol{y}_k = \boldsymbol{z}_k + \boldsymbol{v}_k, \quad \boldsymbol{v}_k \sim \mathcal{N}_{iid}(0, R). \tag{6c}$$

$\boldsymbol{x}$ is the system state, u is the system input. $\boldsymbol{z}$ and $\boldsymbol{y}$ are the system output and the measurement, respectively. The initial state is assumed to be normally distributed, $\boldsymbol{x}_0 \sim \mathcal{N}(\bar{x}_0, P_0)$. $\boldsymbol{w}_k$ and $\boldsymbol{v}_k$ indicates the process and the measurement noises. Q and R indicate the process and measurement noise covariance. (A, B, G, C, Q, R) are computed from the transfer function representation (4)-(5). The discrete-time state space model (6) is used as the simulation model. The model used for control is (6) augmented with integrators to have offset free control.

3. STATE ESTIMATION

In this section, we present a linear Kalman filter with memory for handling missing and delayed observations. The proposed Kalman filter can estimate system states using delayed laboratory measurements such as Y_2.

3.1 Dynamic Kalman filter

The Kalman filter is initialized with the mean and covariance of the initial state

$$\hat{x}_{0|0} = \bar{x}_0, \tag{7a}$$

$$P_{0|0} = P_0. \tag{7b}$$

[2] We use the MPC toolbox from 2-control ApS.

Algorithm 1: Dynamic Kalman filter with memory.

Data:
$\mathcal{Y}_k$, $\mathcal{F}_k$, $\mathcal{U}_k$, N_{mem},
$(\hat{x}_{k-N_{mem}|k-N_{mem}}, P_{k-N_{mem}|k-N_{mem}})$.
for $i = 1 : N_{mem}$ **do**
  One-step prediction. Use (8) to compute
  $(\hat{x}_{k-N_{mem}+i|k-N_{mem}+i-1}, P_{k-N_{mem}+i|k-N_{mem}+i-1})$
  Filtering. Define
  $y_{k-N_{mem}+i}$, $C_{k-N_{mem}+i}$, $R_{k-N_{mem}+i}$,
  as in (14) and use (9)-(11) to compute
  $(\hat{x}_{k-N_{mem}+i|k-N_{mem}+i}, P_{k-N_{mem}+i|k-N_{mem}+i})$.
end
Result: $(\hat{x}_{k|k}, P_{k|k})$

Time update:
In the time update, the mean and covariance are computed using the linear system dynamics, as

$$\hat{x}_{k+1|k} = A\hat{x}_{k|k} + Bu_k, \tag{8a}$$

$$P_{k+1|k} = AP_{k|k}A' + GQG', \tag{8b}$$

Measurement update:
In the measurement update, we compute the innovation and its covariance as

$$e_k = y_k - \hat{y}_{k|k-1}, \tag{9a}$$

$$R_{e,k} = C_k P_{k|k-1} C_k' + R_k, \tag{9b}$$

where $\hat{y}_{k|k-1} = C_k \hat{x}_{k|k-1}$. The Kalman gain is computed as

$$K_{f_x,k} = P_{k|k-1} C_k' R_{e,k}^{-1}. \tag{10}$$

The mean and covariance estimates are computed as

$$\hat{x}_{k|k} = \hat{x}_{k|k-1} + K_{f_x,k} e_k, \tag{11a}$$

$$P_{k|k} = (I - K_{f_x,k}C_k)\, P_{k|k-1}\, (I - K_{f_x,k}C_k)' + K_{f_x,k} R_k K_{f_x,k}', \tag{11b}$$

where (11b), Joseph stabilizing form, is numerically stable.

3.2 Dynamic Kalman filter with memory

The dynamic Kalman filter with memory estimates the states over a horizon of past observations. At any point in time, the memory can be updated with available observations, current or delayed, e.g., laboratory measurements. We define an integer N_{mem} indicating the length of the memory, the horizon of the past observations $\mathcal{Y}$, a boolean matrix $\mathcal{F}$ indicating the availability of observations at any point over the horizon, and the horizon of the past inputs $\mathcal{U}$ as

$$\mathcal{Y}_k = \begin{bmatrix} | & | & & | \\ y_{k-N_{mem}+1} & y_{k-N_{mem}+2} & \cdots & y_k \\ | & | & & | \end{bmatrix}, \tag{12a}$$

$$\mathcal{F}_k = \begin{bmatrix} | & | & & | \\ f_{k-N_{mem}+1} & f_{k-N_{mem}+2} & \cdots & f_k \\ | & | & & | \end{bmatrix}, \tag{12b}$$

$$\mathcal{U}_k = \begin{bmatrix} | & | & & | \\ u_{k-N_{mem}} & u_{k-N_{mem}+1} & \cdots & u_{k-1} \\ | & | & & | \end{bmatrix}. \tag{12c}$$

Additionally, we store the estimated state mean and covariance required for state estimation over the horizon of past observations in each iteration

$$\hat{x}_{k-N_{mem}|k-N_{mem}}, \qquad P_{k-N_{mem}|k-N_{mem}}. \tag{13}$$

At each point in the state estimation over the horizon, the boolean matrix is used to slice the relevant vectors and matrices to the right size, such that

$$y_{k-N_{mem}+i} = \mathcal{Y}_k[\mathcal{F}_k[:,i],i], \tag{14a}$$
$$C_{k-N_{mem}+i} = C[\mathcal{F}_k[:,i],:], \tag{14b}$$
$$R_{k-N_{mem}+i} = R[\mathcal{F}_k[:,i],\mathcal{F}_k[:,i]], \tag{14c}$$

for $i \in \{1,2,\ldots,N_{mem}\}$, i.e., only the relevant rows and columns of the matrices, corresponding to the available observations, are used in the state estimation. If at any point a delayed observation becomes available, it is stored at the relevant position in $\mathcal{Y}_k$ and the corresponding boolean vector elements in $\mathcal{F}_k$ are changed from 0 to 1, indicating that the observations should be included in the state estimation. In each step, the state estimation is performed using Algorithm 1.

4. OPTIMIZATION FOR BLENDING PROCESSES

This section introduces the LMPC and the NMPC for the raw mix blending process. A novel formulation for the LMPC is presented.

4.1 Compositional parameters

The compositional parameters LSF, ALM, and SIM can be computed from the oxide component concentrations,

$$\mathcal{L}(t) = \frac{100\mathrm{Ca}(t)}{2.8\mathrm{Si}(t) + 1.18\mathrm{Al}(t) + 0.65\mathrm{Fe}(t)}, \tag{15a}$$
$$\mathcal{A}(t) = \frac{\mathrm{Al}(t)}{\mathrm{Fe}(t)}, \tag{15b}$$
$$\mathcal{S}(t) = \frac{\mathrm{Si}(t)}{\mathrm{Al}(t) + \mathrm{Fe}(t)}. \tag{15c}$$

Si(t), Al(t), Fe(t), Ca(t) are the concentrations of oxide components in weight percentage. A fractional-form quality function $q(z(t))$ is introduced to express the nonlinear compositional parameters,

$$q_{n,k} = q_n(z_k) = \frac{b_n' z_k + \beta_n}{a_n' z_k + \alpha_n}, \quad n \in \{\mathcal{L},\mathcal{A},\mathcal{S}\}, \tag{16a}$$
$$q_k = q(z_k) = \begin{bmatrix} q_{\mathcal{L},k} \\ q_{\mathcal{A},k} \\ q_{\mathcal{S},k} \end{bmatrix}. \tag{16b}$$

$b_n \in \mathbb{R}^{n_z}$ and $a_n \in \mathbb{R}^{n_z}$ are two constant vectors. β_n and α_n are two scalars. In the raw mix blending optimal control problem, the compositional parameters need to follow the given targets while satisfying constraints. The set point of the compositional parameters is denoted as $\bar{q} = [\bar{\mathcal{L}}; \bar{\mathcal{A}}; \bar{\mathcal{S}}]$. The upper and lower bounds of the compositional constraints are denoted as $q_{\max} = [\mathcal{L}_{\max}; \mathcal{A}_{\max}; \mathcal{S}_{\max}]$ and $q_{\min} = [\mathcal{L}_{\min}; \mathcal{A}_{\min}; \mathcal{S}_{\min}]$.

4.2 Nonlinear blending MPC

The optimal control problem considered in the NMPC is defined as

$$\min_{\{u_i,s_{i+1},t_{i+1}\}_{i=0}^{N-1}} \phi = \phi_q + \phi_s + \phi_t + \phi_{eco} + \phi_{\Delta u} \tag{17a}$$
$$s.t. \qquad x_0 = \hat{x}_{k|k}, \tag{17b}$$
$$x_{i+1} = Ax_i + Bu_i, \qquad i \in \mathcal{N}, \tag{17c}$$
$$z_{i+1} = Cx_{i+1}, \qquad i \in \mathcal{N}, \tag{17d}$$
$$e'u_i = 1, \qquad i \in \mathcal{N}, \tag{17e}$$
$$u_{\min,i} \le u_i \le u_{\max,i}, \qquad i \in \mathcal{N}, \tag{17f}$$
$$\Delta u_{\min,i} \le \Delta u_i \le \Delta u_{\max,i}, \; i \in \mathcal{N}, \tag{17g}$$
$$q_{i+1} = q(z_{i+1}), \qquad i \in \mathcal{N}, \tag{17h}$$
$$q_{i+1} \le q_{\max,i+1} + t_{i+1}, \qquad i \in \mathcal{N}, \tag{17i}$$
$$q_{i+1} \ge q_{\min,i+1} - s_{i+1}, \qquad i \in \mathcal{N}, \tag{17j}$$
$$s_{i+1} \ge 0, \; t_{i+1} \ge 0, \qquad i \in \mathcal{N}, \tag{17k}$$

where $\mathcal{N} = \{0,1,\ldots,N-1\}$ for N indicating the prediction and control horizons of the NMPC. In the blending optimal control problem, we consider the reference tracking objective ϕ_q, the soft constraint penalty objectives ϕ_s and ϕ_t, the economic objective ϕ_{eco}, as well as the input rate of movement (ROM) objective ϕ_{Δ_u}. They are denoted as

$$\phi_q = \alpha_q \sum_{i=0}^{N-1} \frac{1}{2} \left\| W_q(q_{i+1} - \bar{q}_{i+1}) \right\|_2^2, \tag{18a}$$
$$\phi_s = \alpha_s \sum_{i=0}^{N-1} \frac{1}{2} \left\| W_s s_{i+1} \right\|_2^2 + q_s' s_{i+1}, \tag{18b}$$
$$\phi_t = \alpha_t \sum_{i=0}^{N-1} \frac{1}{2} \left\| W_t t_{i+1} \right\|_2^2 + q_t' t_{i+1}, \tag{18c}$$
$$\phi_{eco} = \alpha_{eco} \sum_{i=0}^{N-1} c' u_i, \tag{18d}$$
$$\phi_{\Delta u} = \alpha_{\Delta u} \sum_{i=0}^{N-1} \frac{1}{2} \left\| W_{\Delta u} \Delta u_i \right\|_2^2. \tag{18e}$$

in which $W_q, W_s, W_t, W_{\Delta u}, q_s$, and q_t are scaling factors. $\alpha_q + \alpha_s + \alpha_t + \alpha_{eco} + \alpha_{\Delta u} = 1$ for $\alpha_q, \alpha_s, \alpha_t, \alpha_{eco}, \alpha_{\Delta u} \ge 0$ indicate the weights of objectives. c is the unit cost vector of the raw material piles. $u_{\min}$, $u_{\max}$, $\Delta u_{\min}$, and $\Delta u_{\max}$ are the input and the input ROM hard constraints. s and t are slackness variables for softening the compositional parameter constraints.

4.3 Linear blending MPC

The nonlinearity in the optimal control problem (17) appears as q_k is nonlinear in z_k. Consider a reference tracking problem on a quality function (16),

$$\begin{aligned} \phi_{q,n} &= \sum_{i=0}^{N-1} \frac{1}{2} \left\| W_q(q_{n,i+1} - \bar{q}_{n,i+1}) \right\|_2^2 \\ &= \sum_{i=0}^{N-1} \frac{1}{2} \left\| W_q \epsilon_{n,i+1} \right\|_2^2, \end{aligned} \tag{19}$$

where $n \in \{\mathcal{L},\mathcal{A},\mathcal{S}\}$. $\bar{q}_n$ indicates the set point of the compositional parameter n. The residual function $\epsilon_{n,i+1}$ is

$$\begin{aligned} \epsilon_{n,i+1} &= q_{n,i+1} - \bar{q}_n \\ &= \frac{(b_n' - \bar{q}_n a_n')z_{i+1} + \beta_n - \bar{q}_n \alpha_n}{a_n' z_{i+1} + \alpha_n}, \end{aligned} \tag{20}$$

By multiplying the denominator of (20) on both side, a new residual function can be defined as

$$\begin{aligned} \tilde{\epsilon}_{n,i+1} &= (a_n' z_{i+1} + \alpha_n)\epsilon_{n,i+1} \\ &= (b_n' - \bar{q}_n a_n')z_{i+1} + \beta_n - \bar{q}_n \alpha_n \\ &= M_n z_{i+1} + m_n, \end{aligned} \tag{21}$$

where $M_n = b'_n - \bar{q}_n a'_n$ and $m_n = \beta_n - \bar{q}_n \alpha_n$. Consequently, we can formulate an approximation to the reference tracking objective (19) as

$$\bar{\phi}_{q,n} = \sum_{i=0}^{N-1} \frac{1}{2} \left\| \bar{W}_q (M_n z_{i+1} + m_n) \right\|_2^2, \tag{22}$$

The value of (21) will be zero when the error between the set point $\bar{q}_{n,i+1}$ and $q_n(z_{i+1})$ is zero. We can use this feature to minimize the reference tracking objective. Therefore, a quadratic objective for the reference tracking objective can be defined as

$$\bar{\phi}_q = \alpha_q \sum_{i=0}^{N-1} \frac{1}{2} ||W_q (M_q z_{i+1} + m_q)||_2^2, \tag{23a}$$

$$M_q = \begin{bmatrix} M_{\bar{\mathcal{L}}} \\ M_{\bar{\mathcal{A}}} \\ M_{\bar{\mathcal{S}}} \end{bmatrix} = \begin{bmatrix} -2.8\bar{\mathcal{L}} & -1.18\bar{\mathcal{L}} & -0.56\bar{\mathcal{L}} & 100 \\ 0 & 1 & -\bar{\mathcal{A}} & 0 \\ 1 & -\bar{\mathcal{S}} & -\bar{\mathcal{S}} & 0 \end{bmatrix}, \tag{23b}$$

$$m_q = \begin{bmatrix} m_{\bar{\mathcal{L}}} \\ m_{\bar{\mathcal{A}}} \\ m_{\bar{\mathcal{S}}} \end{bmatrix} = \begin{bmatrix} 0 \\ 0 \\ 0 \end{bmatrix}, \tag{23c}$$

Similarly, we can reformulate the nonlinear compositional parameter inequality constraint (17i) with the same method. By multiplying the denominator of the quality function $q(z(t))$ on both sides of (17i), we can obtain a linear inequality constraint as

$$q_{i+1} \leq q_{\max,i+1} + t_{i+1}, \quad M_{q,\max} z_{i+1} \leq m_{q,\max} + t_{i+1}, \tag{24a}$$

$$q_{i+1} \geq q_{\min,i+1} - s_{i+1}, \quad M_{q,\min} z_{i+1} \leq m_{q,\min} - s_{i+1}, \tag{24b}$$

where

$$M_{q,\max} = \begin{bmatrix} -2.8\mathcal{L}_{\max} & -1.18\mathcal{L}_{\max} & -0.56\mathcal{L}_{\max} & 100 \\ 0 & 1 & -\mathcal{A}_{\max} & 0 \\ 1 & -\mathcal{S}_{\max} & -\mathcal{S}_{\max} & 0 \end{bmatrix}, \tag{25a}$$

$$M_{q,\min} = -\begin{bmatrix} -2.8\mathcal{L}_{\min} & -1.18\mathcal{L}_{\min} & -0.56\mathcal{L}_{\min} & 100 \\ 0 & 1 & -\mathcal{A}_{\min} & 0 \\ 1 & -\mathcal{S}_{\min} & -\mathcal{S}_{\min} & 0 \end{bmatrix}, \tag{25b}$$

In this case, $m_{q,\min} = m_{q,\max} = 0$ since the compositional parameters have no constant term. It should be noticed that this reformulation method only works when the sign of the denominator is constant (positive or negative).

With (23) and (24), a convex QP for the LMPC can be defined as

$$\min_{\{u_i, s_{i+1}, t_{i+1}\}_{i=0}^{N-1}} \phi = \bar{\phi}_q + \phi_s + \phi_t + \phi_{eco} + \phi_{\Delta u} \tag{26a}$$

$$\begin{aligned}
s.t. \quad & x_0 = \hat{x}_{k|k}, && && (26b)\\
& x_{i+1} = Ax_i + Bu_i, && i \in \mathcal{N}, && (26c)\\
& z_{i+1} = Cx_{i+1}, && i \in \mathcal{N}, && (26d)\\
& e'u_i = 1, && i \in \mathcal{N}, && (26e)\\
& u_{\min} \leq u_i \leq u_{\max}, && i \in \mathcal{N}, && (26f)\\
& \Delta u_{\min} \leq \Delta u_i \leq \Delta u_{\max}, && i \in \mathcal{N}, && (26g)\\
& M_{q,\max} z_{i+1} \leq t_{i+1}, && i \in \mathcal{N}, && (26h)\\
& M_{q,\min} z_{i+1} \leq s_{i+1}, && i \in \mathcal{N}, && (26i)\\
& s_{i+1} \geq 0,\ t_{i+1} \geq 0, && i \in \mathcal{N}, && (26j)
\end{aligned}$$

where the objectives $\phi_s, \phi_t, \phi_{eco}$, and $\phi_{\Delta u}$ are the same as in the objective functions (18b) - (18e) for the optimal control problem in the NMPC.

5. SIMULATION RESULTS

In this section, we test and compare the LMPC and NMPC on the simulated raw mix blending model described in Section 2. The sampling time is $T_s = 5$ [min]. The prediction and control horizons are selected as $N = 50$. The simulated blending process has four raw material piles. The time delay of input piles are $\tau_{D1} = [0.55, 0.50, 0.45, 0.40]$ [min]. The composition matrix P and the cost vector c are

$$P = \begin{bmatrix} 65.0 & 2.10 & 1.40 & 0.90 \\ 1.80 & 15.9 & 2.20 & 4.10 \\ 0.10 & 1.30 & 32.6 & 0.20 \\ 0.50 & 0.40 & 2.80 & 62.40 \end{bmatrix}, \quad c = \begin{bmatrix} 550.0 \\ 1600.0 \\ 935.0 \\ 1145.0 \end{bmatrix}. \tag{27}$$

The time delay of G_{D2} is $\tau_{D2} = 20$ [min]. We assume that the laboratory measurement Y_2 is available every 60 [min]. The measurement covariance is selected as $R = \text{diag}([10^{-1}e; 10^{-3}e])$, $e = [1; 1; 1; 1]$. The input and input ROM hard constraints are $u_{\min} = 0, u_{\max} = 1$ and $\Delta u_{\min} = -0.5, \Delta u_{\max} = 0.5$ for all piles. The compositional parameter constraints are $\mathcal{L}_{\min} = 92, \mathcal{L}_{\max} = 98, \mathcal{A}_{\min} = 1.0, \mathcal{A}_{\max} = 2.5, \mathcal{S}_{\min} = 2.3$, and $\mathcal{S}_{\max} = 2.7$. The set point for LSF is $\bar{\mathcal{L}} = 95.0$, and it changes to $\bar{\mathcal{L}} = 90.0$ at $t > 6$ [h]. Similarly, the constraints of the LSF are changed to $\mathcal{L}_{\min} = 87$, and $\mathcal{L}_{\max} = 93$. We do not consider set points for ALM and SIM. Therefore, the scaling factors of the reference tracking objectives are $W_q = \text{diag}([10^1; 0; 0])$ and $\bar{W}_q = \text{diag}([2.6; 0; 0])$. Other scaling factors are selected as $W_s = W_t = \text{diag}([10^3; 10^3; 10^3]), W_{\Delta u} = \text{diag}([10^1; 10^1; 10^1; 10^1])$ and $q_s = q_t = [10^3; 10^3; 10^3]$. The weighting parameters are selected as $\alpha_q = \alpha_s = \alpha_t = \alpha_{eco} = \alpha_{\Delta u} = 0.2$, such that all objectives are treated equally.

Based on the model identification method described in Prasath et al. (2013), we can obtain a control-oriented model for MPCs,

$$\hat{\boldsymbol{Y}}(s) = \hat{G}(s)U(s) + \hat{H}(s)\boldsymbol{E}(s), \tag{28}$$

where $\hat{G}(s)$ and $\hat{H}(s)$ are the deterministic and stochastic transfer functions. A gain mismatch matrix $G_m = \text{diag}([1.1; 0.95; 0.90; 1.05])$ is introduced as $\hat{G}(s) = G(s)\, G_m(s)$, representing the variations of the input pile compositions. The control model is realized to a discrete-time state space model, which is used in the MPCs and the Kalman filters. To compare the performances of the MPCs, we test the MPCs on the same simulation model with the same parameters. We use CasADi to solve the optimization problem of the NMPC, and the LMPC is solved by using the MATLAB function `quadprog`. Several performance indicators are introduced for quantifying the controller performance. The time-outside-range parameter $T_i[\%]$ for $i \in \{\mathcal{L}, \mathcal{A}, \mathcal{S}\}$ indicates the percentage of samples for which the parameter i violates boundaries. $T_{CPU}[s]$ is the average computation time and cost [\$/t] is the average piles cost. The initial input is $u_0 = [0.25; 0.25; 0.25; 0.25]$ and the initial states are steady states. An unknown disturbance $d = [8.0; 8.0; 8.0; 20] \cdot 10^{-2}$ is added to u during the simulation.

Figure 2 illustrates the closed-loop simulation results. We notice that the NMPC and the LMPC perform similarly for the three compositional parameters. This indicated that the LMPC approximates the NMPC well, which is reasonable since the dynamics and the objective functions

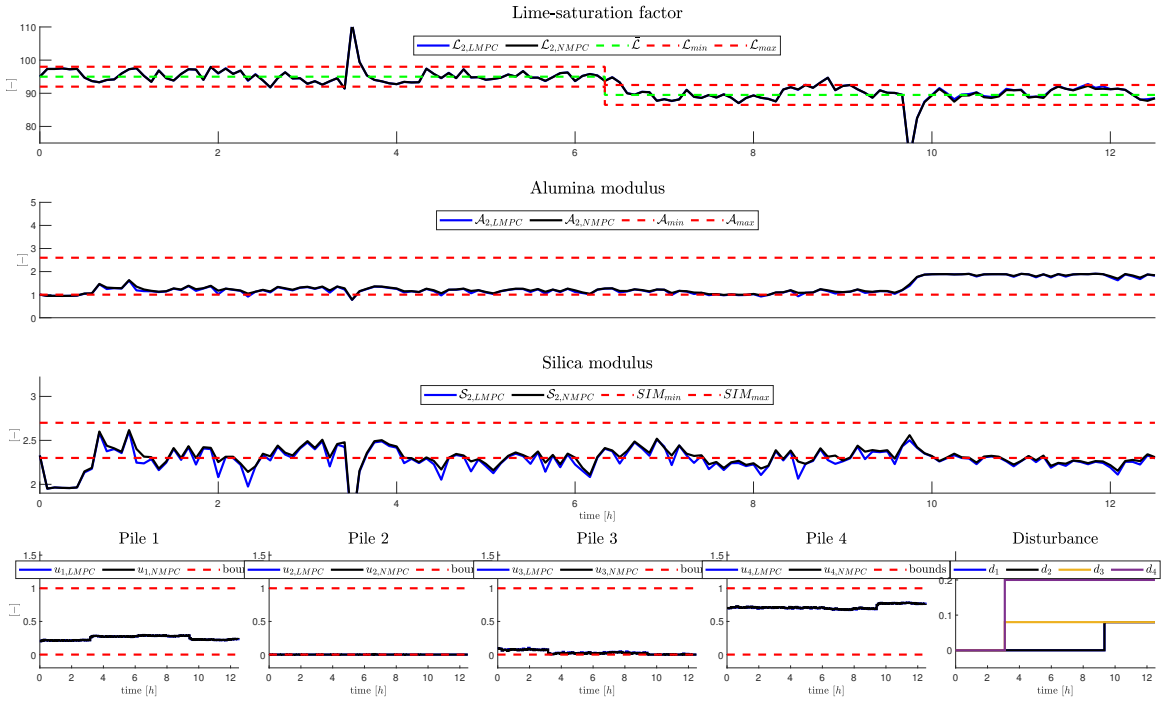

Fig. 2. The closed-loop simulation results of the LMPC and NMPC on a simulated raw mix blending process. Three compositional parameters LSF, ALM, and SIM are shown in the plot. The green line indicates the set point for LSF. Red dashed lines are boundaries. The blue lines indicate the true value of the LMPC. The black lines are the true value of the NMPC. The last row of figures are the system inputs and the unknown disturbance.

Table 1. KPIs for the LMPC and the NMPC.

	$T_{\mathcal{L}}$	$T_{\mathcal{A}}$	$T_{\mathcal{S}}$	T_{CPU}	Cost
LMPC	9.27	10.60	56.95	6.04	990.10
NMPC	7.28	7.28	42.38	8.55	989.99

of the MPCs are designed with this property in mind. At the beginning, both MPCs take some time to bring the system to the target area. This indicates that the MPCs can handle plant-model mismatch. Two significant overshoots caused by unknown disturbance d occur at $t \in \{3, 10\}$ [h]. After a few iterations, the two overshoots disappear, indicating that the MPCs can reject unknown disturbances. The reference point and constraints of the LSF are changed at $t = 6$ [h], and both MPCs follow the new target and satisfy the constraints. There are slight differences between the LMPC and NMPC on ALM and SIM. We consider this phenomenon normal, since the optimal control problems are not exactly equivalent. The inputs of the MPCs show similar trends.

Table 1 displays the key performance indicators for the NMPC and the LMPC. The LMPC and NMPC have similar performances regarding the time-in-range performance metrics, $T_{\mathcal{L}}$, $T_{\mathcal{A}}$ and $T_{\mathcal{S}}$. As expected, the NMPC performs slightly better than the LMPC on the time-in-range metrics as well as the cost. The average costs related to both MPCs are around 990 [$/$t$]. As expected the the LMPC is slighlty more computationally efficient than the NMPC. The average CPU times of the LMPC and the NMPC are both less than 10 seconds, which is much smaller than the sampling time of 5 min. The computational time may be further optimized, by tailoring the optimization algorithm to the special problem structure.

6. CONCLUSION

For controlling the output raw meal quality of the raw mix blending process, LMPC and NMPC using a Kalman filter with memory are described. The simulation results indicate that both MPCs can stabilize and control the simulated raw mix blending process well. The proposed NMPC and LMPC have similar performance and are both computationally feasible. Consequently, both the NMPC and the LMPC can be used for cement blending control. We recommend the NMPC.

REFERENCES

Prasath, G., Recke, B., Chidambaram, M., and Jørgensen, J.B. (2010). Application of soft constrained mpc to a cement mill circuit. In *Proceedings of the 9th IFAC Symposium on Dynamics and Control of Process Systems*, 302–307. Leuven, Belgium.

Prasath, G., Recke, B., Chidambaram, M., and Jørgensen, J.B. (2013). Soft constrained based mpc for robust control of a cement grinding circuit. In *Proceedings of the 10th IFAC International Symposium on Dynamics and Control of Process Systems*, 475–480. Mumbai, India.

Robbie, A.M. (2019). Global CO_2 emissions from cement production, 1928-2018. *Earth System Science Data*, 11(4), 1675–1710.

Vinicius, D.O., Michael, A., and Alireza, K. (2015). Robust gain-scheduled blending control of raw-mix quality in cement industries. In *Proceedings of the 50th IEEE Conference on Decision and Control*, 4189–4194. Orlando, FL, USA.